

Division - Soil Processes and Properties | Commission - Soil Physics

Analysis of changes in volume and propagation of cracks in expansive soil due to changes in water content

Silvio Romero de Melo Ferreira^{(1)*} , Arthur Gomes Dantas de Araújo^{(1),(2)} , Felipe Araújo Silva Barbosa⁽¹⁾ , Thalita Cristina Rodrigues Silva⁽¹⁾  and Izabela Medeiros de Lima Bezerra⁽¹⁾ 

⁽¹⁾ Universidade Federal de Pernambuco, Departamento de Engenharia Civil e Ambiental, Programa de Pós-Graduação em Engenharia Civil, Recife, Pernambuco, Brasil.

⁽²⁾ Universidade Federal Rural do Semi-Árido, Departamento de Engenharias, Angicos, Rio Grande do Norte, Brasil.

ABSTRACT: Expansive clay soils are a problem for agriculture and engineering because they are susceptible to change in volume due to seasonal variation in water content and temperature. One of its morphological properties is slickensides, which result from the ability to contract and crack when dry and expand by wetting. The objective of this study was to evaluate the processes of expansion and formation and propagation of cracks due to the change in water content over time. The expansion process was evaluated through simple edometric tests with different external stress values applied to undisturbed soil samples. To evaluate the shrinking process, a device was developed to monitor the process of crack propagation. The mechanisms through which cracks begin and develop were studied using molded soil samples at the liquidity limit and at 1.25 times the liquidity limit with a drying and wetting cycle. Crack initiation conditions and development of geometric crack indices were measured with the water content and drying time. The soil presented medium to high expansion that depends on the overburden and suction applied, and the swelling stress was found to increase as suction increases. The changes in volume due to wetting and the propagation of cracks due to drying developed in three stages: initial, primary, and secondary. In the initial stage, few cracks or swelling occur with gradual variation in water content. As the water content approaches the limit of soil contraction (in the drying process) or the limit of soil saturation (in the wetting process), cracks and expansion developed slowly and approach a secondary stage. In the primary stage, cracks and expansion occurred rapidly with drying or wetting, respectively. Drying and wetting cycles showed similar crack patterns with the appearance of new micro-cracks during each new drying cycle.

Keywords: cracking, unsaturated soils, desertification, soil conservation, soil mechanics.

* **Corresponding author:**
E-mail: sr.mf@hotmail.com

Received: December 11, 2019

Approved: September 14, 2020

How to cite: Ferreira SRM, Araújo AGD, Barbosa FAS, Silva TCR, Bezerra IML. Analysis of changes in volume and propagation of cracks in expansive soil due to changes in water content. Rev Bras Cienc Solo. 2020;44:e0190169.
<https://doi.org/10.36783/18069657rbc20190169>

Copyright: This is an open-access article distributed under the terms of the Creative Commons Attribution License, which permits unrestricted use, distribution, and reproduction in any medium, provided that the original author and source are credited.



INTRODUCTION

Expansive soils have attracted the attention of scientists in many countries because of their unusual properties, expanding when moistened and contracting and cracking when dried. Investigations have been developed to understand and explain their characteristics and properties (Chen, 1988; Ferreira and Ferreira, 2009; Marques et al., 2014). These behaviors are not avoidable because there is a set of intrinsic factors inherent to the soil itself (clay particle distribution, structure, mineralogical orientation, cementation, stratigraphic profile, soil thickness, lithological discontinuity, etc.) that establish the potential expansive capacity and other external factors such as climate, water availability, biota, and anthropic action (management, use, and occupation) that determine whether or not the expansive potential is realized (Chen, 1988; Corrêa et al., 2003; Ferreira and Ferreira, 2009).

Expansive soils are developed from parent material rich in calcium and magnesium, with an expansive clay mineral, high activity, low drainage, and found in semi-arid, tropical, and temperate climates. They are found among Chernosols, Luvisols, Nitisols, Planosols, and Vertisols (Antunes and Salomão, 2018). The main difficulty in the use of expansive soil is the proper management of water in agricultural practices. These soils have horizons with a high level of type 2:1 clay minerals which, when moistened, increase in volume due to the entry of water within their structure, making them plastic and sticky. When dry, they have a hard consistency, forming internal clusters and surface cracks (Biassusi et al., 1999). In agriculture, plowing and lack of vegetation cover or dead cover expose the soil to more dryness. Consideration must also be given to the densification caused by machinery and animal trampling when grazing, in addition to surface sealing due to the impact of rain (Flores et al., 2007; Collares et al., 2008; Moraes et al., 2011). However, when this land is used for construction or requires engineering structures such as irrigation canals and agrovillages, special attention is required, as the implantation of a structure inevitably modifies the field soil water content (Al-Rawas et al., 2006; Al-Mukhtar et al., 2012; Liu et al., 2014; Lim and Siemens, 2016; Yuan et al., 2016).

The volume change in expansive clays due to changes in applied external stresses or suction is influenced by the presence of water bound to the solid part of the mineral clay, associated with the presence of adsorbed water and the double layer (Lambe and Whitman, 1969; Mitchell, 1976). The expansion mechanism can be explained by the attraction of clay particles, hydration of cations, and osmotic repulsion. The negative electrical charge on the surface of the clay particle generates attractive forces, which attract cations and polar molecules (for example, water) and acts as a fixing force on the water of the double layer. The volume of water increases until there is a sufficient volume variation in the soil mass, since the force of water adsorption by the particle decreases with increasing distance to the surface. In cation hydration, the negative surface of the clay particle attracts cations that cancel its negative charge. Some cations after neutralizing the negative charge of the clay particle remain with an amount of non-neutralized charge, attracting water molecules through the negative poles, which through their positive poles attract other water molecules. The osmotic repulsion the moment the clay-water-cations system is placed in contact with water in a lower ionic concentration, the double layer boundary acts as a semipermeable membrane. Water tends to pass this membrane to equalize, by osmosis, the concentrations on both sides of the membrane. This increases the thickness of the double layer and in the volume of soil mass.

The contraction and cracking mechanism of saturated clay by drying the water film on the surface evaporates first and the structure and the state of tension - deformation of the soil are practically unaffected. As the water-air interface reaches the surface of the soil layer, the formation of a meniscus begins, capillary suction begins to develop, the clay layer compresses, and contracts. The continuation of evaporation increases

the curvature of the capillary meniscus and thus increases the capillary suction and the effective tension between the clay particles. When these stresses exceed the soil's tensile strength, they appear at the first cracks (Tang et al., 2011a).

The formation and propagation of cracks in the soil is a natural process caused by dryness that results from seasonal environmental variations, with alternating dry and wet periods. During the dry periods, the soil retracts, forming cracks. The presence of desiccation cracks in the soil alters its mechanical and hydraulic properties (Lloret et al., 1998; Nahlawi and Kodikara, 2006; Li and Zhang, 2011; Tang et al., 2011b; Li et al., 2012; Shi et al., 2014; Chaduvula et al., 2017). In addition to leachate infiltration into compacted landfills, the crack reduces resistance, creates preferential flow, and increases the infiltration rate (Albrecht and Benson, 2001; Albright et al., 2006; Tang et al., 2011a; Ghazizade and Safari, 2017). In civil engineering, the presence of cracks causes negative impacts on layers whose main purpose is waterproofing. These cracks alter the flow conditions and mechanical behavior, compromising layers, pavement, and canals, which can cause accidents and contaminate underground water systems, generating economic losses and damage to public health (Rodríguez et al., 2007; Cotecchia and Vitone, 2015).

Several studies have been developed to interpret the behavior of expansive clays on the development of cracks during drying/wetting cycles, with temperature and geometric variation of the sample, using digital image analysis and computational numerical modeling (Lakshmikantha et al., 2009; Li and Zhang, 2010; Atique and Sanchez, 2011; Tang et al., 2010, 2011c, 2019; Sánchez et al., 2014; Shi et al., 2014; Fleureau et al., 2015; Ammour and Bouhanna, 2016; Chaduvula et al., 2016, 2017; Julina and Thyagaraj, 2018).

The behavior of volume change for expansive soil is influenced by the drying process, the wetting process, and any applied stress. The present study seeks to evaluate the variation in volume and propagation of cracks in expansive soil due to the increase or decrease in water quantity and analyze the phases of volume increase and crack propagation over time and with drying and wetting cycles.

MATERIALS AND METHODS

Soil samples were taken from the municipality of Paulista (Pernambuco, Brazil) with coordinates: Latitude: 07.00° 55.00' 35.00" - S; Longitude: 34.00° 50.00' 49.00" - W. The soil consists of 470 g kg⁻¹ of clay, 250 g kg⁻¹ of silt, and 28 g kg⁻¹ of sand. The liquidity limit is 76 %, plasticity limit is 30 %, and the grain density (G) of the soil is equal to 2.674. The soil originates from the physical-chemical weathering of clay and limestone from the Maria Farinha Formation (Bastos, 1994). The local climate is hot and humid tropical with an accentuated dry period of 7 to 8 months, being classified as As' according to the criteria of Köppen and Geiger. The average annual temperature at the sampling site is 26 °C and the average annual rainfall is 1819 mm (Climate-Data.org, 2019). The soil is acidic [pH(H₂O) 4.93], eutrophic (V value = 56.80 %), highly active (T = 40.92 cmol_c kg⁻¹) and has irregular interstratification involving 2:1 minerals with micas and expansive minerals (smectites), as well as kaolinite (Ferreira et al., 2017). The study was developed in two stages. In the first stage, tests were performed to evaluate expansiveness due to wetting and in the second, an apparatus was developed to evaluate the process and propagation of cracks during wetting and drying cycles.

Tests to evaluate volume change behavior due to wetting

The volume change behavior due to wetting was analyzed considering the influence of vertical flooding stress. Simple edometric tests were performed on undisturbed samples collected at depths of 1.0 to 1.3 m, cast in thin-walled stainless steel rings with a height of 20.0 mm and a diameter of 71.3 mm. The specimens were loaded at a predetermined vertical stress and subsequently flooded, with compression or expansion deformations

measured. At the beginning of the test, a tension of 1.0 kPa was applied to settle the system and perform the initial reading for the deformation process. The tensions applied during the tests were increased by a value ($\Delta\sigma$) equal to the previously applied tension ($\Delta\sigma/\sigma = 1$), with the initial value being 10 kPa and the final value was 640 kPa.

Soil swelling stress was determined using three methods: (1) loading after expansion with different vertical consolidation stress; (2) expansion and collapse under tension; and (3) constant volume in undisturbed samples, as described by Ferreira and Ferreira (2009). The values for swelling potential (SP) obtained by simple edometric tests were calculated using equation 1.

$$SP = \Delta h \times 100/h_i \quad \text{Eq. 1}$$

in which: SP is the swelling potential, Δh is the variation in specimen height due to flooding, and h_i is the specimen height before flooding.

Undisturbed soil samples were also dried by placing them in vacuum desiccators containing sulfuric acid (H_2SO_4) solutions at different concentrations imposing suctions of 2.0, 8.1, 19.9, 33.2, and 81.1 MPa. Later the samples were placed in edometric cells to determine the swelling stress using the constant volume method.

Tests to evaluate the process and propagation of cracks

To evaluate the propagation of cracks an apparatus was developed that considered the equipment produced by Fleureau et al. (2015) and Ammour and Bouhanna (2016). Figure 1 shows the apparatus with the devices for crack propagation tests designed by the Unsaturated Soil Research Group (GÑSat) at the Federal University of Pernambuco. The assembled apparatus is capable of monitoring ambient temperature, relative air water content, and water content variation of the sample subjected to drying and wetting cycles.

Sample preparation and test procedure

The soil was prepared without any prior air drying and without loosening, beginning from field gravimetric water content ($W = 25\%$) and handled such that the size of lumps was smaller than 2.00 mm. Two tests were performed. Water was added to the soil to reach a water content level close to the liquidity limit (76.10% - Test 1) and 1.25 times the liquidity limit (94.20% - Test 2). The samples were homogenized for uniform water content balance, compacted into 150 mm diameter and 15 mm high Petri dishes with the aid of a plastic socket, which served to spread the soil throughout the mold and remove air bubbles. The soil-plate assembly was placed on a 2.000 g capacity scale with 0.01 g sensitivity. This allowed for the weight of the set to be measured in real-time, and therefore the soil water content could be calculated at any time. The incandescent lamps and laboratory air conditioner were switched on before the start of molding (approximately 2 h before the start of the test itself) to stabilize the initial ambient temperature. In Test 1, only one drying step was performed, lasting 49 h, while in Test 2, three drying and two wetting steps were performed, totaling about 250 h. In Test 2, the wetting cycles were initiated when the soil water content approached the plastic limit in the drying process. To monitor the cracking dynamics of the soil over time, a webcam connected to a notebook computer was used. The images were captured every 10 min, using the free Auto Screenshot Capture software.

Image processing

At the completion of the tests, images were selected that corresponded to the desired water content levels and times. For the drying cycles, images were chosen that corresponded to an approximate 5% variation in gravimetric water content in percentile.

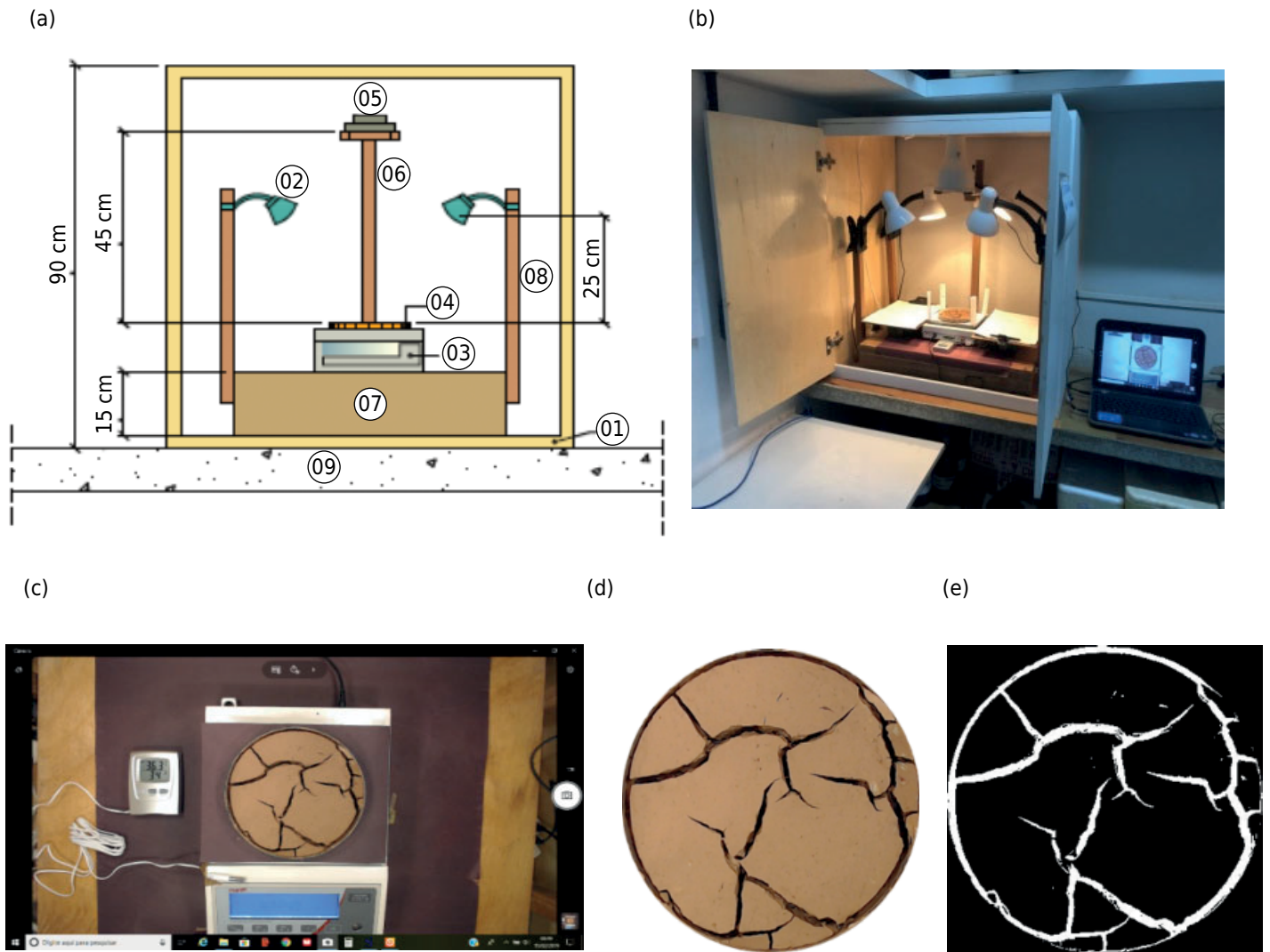


Figure 1. Crack propagation test apparatus. (a) Front view: measures in meters; (b) overview; (c) image selection and cropping process; (d) original color image; (e) binarized image. 01: MDF box; 02: light fixtures; 03: scale with 0.01 g sensitivity; 04: soil-plate Petri assembly; 05: webcam; 06: webcam support rod; 07: wooden base; 08: light fixture support rods; 09: wall.

For the wetting periods, the images were separated by wetting time, with the following reference times adopted: 1, 12, 24, 36, 48, and 70 h. The beginning of the post-wet drying cycles, and consequently the selection of the first image, occurred 24 h after the last water replenishment.

To obtain the most accurate visualization and characterization of the pattern and development of cracks, image processing tools were used. The images were cropped in a circular format, to view only the soil sample. The public domain free software ImageJ was used to perform the binarization process, i.e., transforming the colors of the original image into black and white. Figures 1d and 1e present the comparison between an original color image and a binarized image (Figure 1e), used to quantify the length, width, and the number of crack segments. In addition to cropping and graphical tools, this program can save images in a variety of file extensions. After selecting and cropping the images, the analysis procedure began. In this program, the scale was defined according to the plate diameter, resulting in a value of $2.2075 \text{ pixels mm}^{-1}$.

To quantify crack patterns, the following geometric indices were calculated on each 2D image: (a) Crack Intensity Factor (CIF), which is the ratio of the surface area of the sample that suffered the cracking at any given time compared to the initial surface area of the sample (Equation 2); (b) average crack width, calculated by the shortest distance from

a stochastic point on one edge of a crack segment to the opposite edge; (c) the total crack length, calculated by counting the total number of white pixels after skeletonization of the image; and (d) the number of crack segments, where elements between two adjacent intersections are defined as a crack segment, according to Tang et al. (2019).

$$CIF = Af/At \quad \text{Eq. 2}$$

which: CIF is the crack intensity factor; Af is the surface area of cracks; At is the total initial surface area.

RESULTS

Volume change due to wetting with different overburden is presented in figure 2 showing the curves for specific vertical deformation vs. time (Figure 2a), specific deformation vs. applied vertical stress (σ) (Figure 2b), and swelling potential vs. applied vertical stress (Figure 2c). The values for “free” soil expansion with field water content and small applied stresses of 1 and 10 kPa are 8.00 and 3.49 %, respectively, classifying the soil as having medium expansiveness, according to the criteria of Vijayvergiya and Ghazzaly (1973). The average value for the swelling stress obtained by Method 1 (Loading after expansion with different overloads) is 145 kPa (Figure 2b) and by Method 2 (Expansion and collapse) is 213 kPa (Figure 2c). The value of constant volume swelling stress (Method 3), preventing soil volume variation during the expansion process, is 150 kPa with an average value of 169 kPa.

Formation and propagation of cracks due to drying in Test 1, the soil with initial water content near the liquidity limit (76.1 %) was tested at a temperature of 36.1 ± 0.83 °C, with a coefficient of variation of 0.02 °C and a relative air water content of 36 ± 2.38 %, with a coefficient of variation of 0.07 %. The crack formation process begins within the sample as the soil contracts, radiating through the interior with greater intensity (Figure 3). When the water content decreased from 76.1 % (Figure 3a) to 69.90 % (Figure 3b), the first cracks on the surface of the sample appear after 4.8 h of drying, registering a CIF of 0.6 %. A detachment of the soil from the Petri dish can be seen at 65.20 % water content, with a CIF of 3.80 % (Figure 3c). The pattern of crack that followed appeared simultaneously across the entire soil surface, completely subdividing the initial area. A continual gradual loss of water content leads to crack propagation in different directions, including the creation of forks at various points along the cracks (Figure 3d). The intersecting crack lines are predominantly X- and Y-shaped, forming geometric elements. Primary cracks followed by center-to-edge propagation contributed to the development of the crack surface network (Figures 3e and 3f).

The soil changed color with the sharp desiccation process from 25.10 to 8.3 % water content. Soil color ranged from 5YR 8/4 (“Pink”) to 7YR 5/4 (“Brown”) as water content decreased from its initial value (76.10 %) to its final value (8.30 %), according to the Munsell (1992) color scale. It is important to emphasize that the identification of the soil color was performed in laboratory light based on the images obtained.

Formation and propagation of cracks due to drying in Test 2, the drying process was initiated at 94.2 % water content (equivalent to 1.25 times the liquidity limit), with the temperature range being 33.9 ± 0.59 °C, with a coefficient of variation of 0.02, and a relative air water content of 40 ± 2.47 %, with a coefficient of variation of 0.06. The first drying process was completed after 32.8 h, with a water content of 20.6 % (just above the shrinkage limit), at which point the soil was flooded to observe the behavior of the cracks when wetted. Initially, the crack propagation during the first drying process of Test 2 was compared to Test 1 that began with water content close to the liquidity limit (76.10 %).

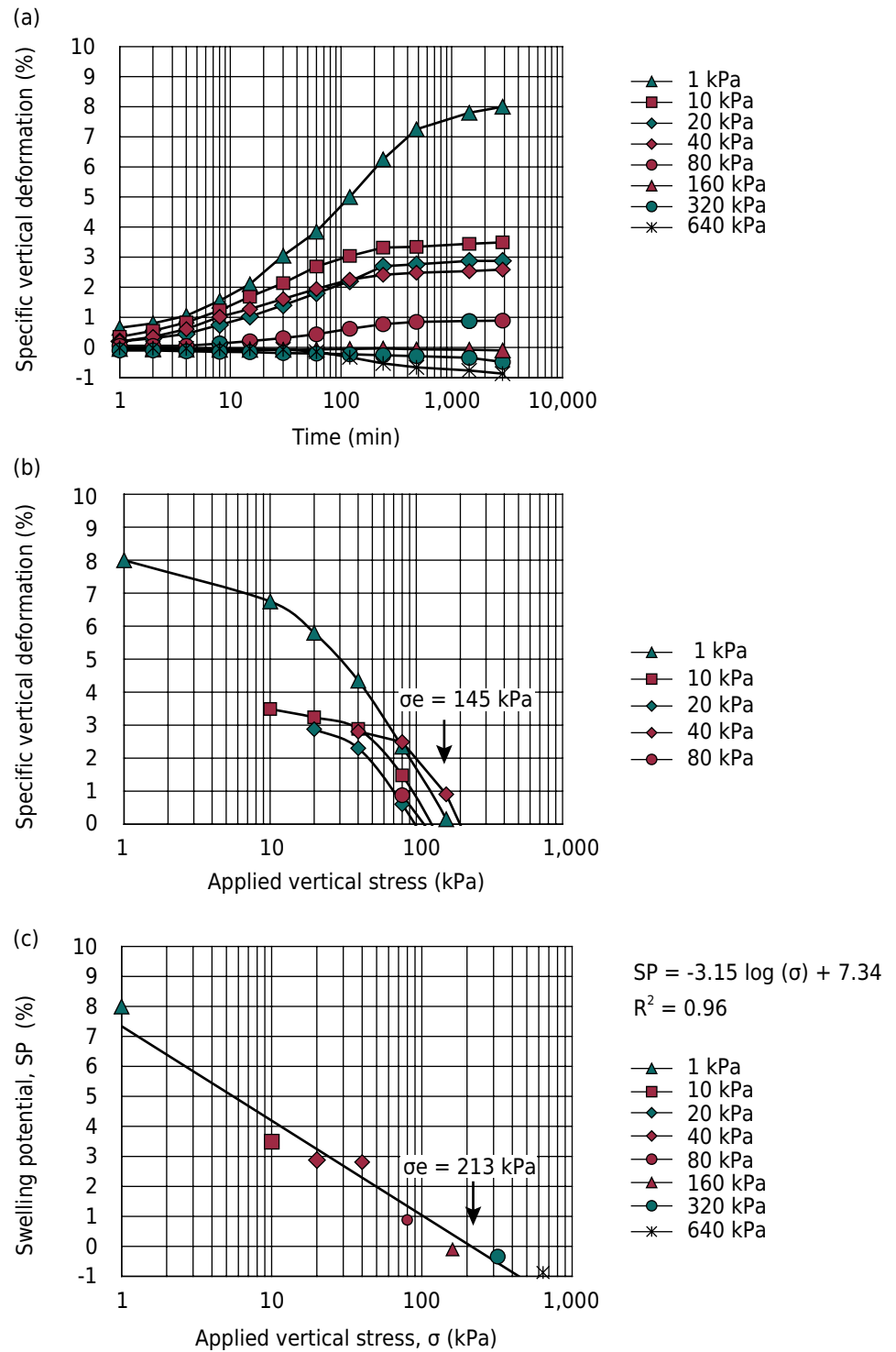


Figure 2. Swelling stress (σ_e): (a) expansion under stress; (b) Method 1: loading after expansion with different vertical consolidation stresses; (c) Method 2: swelling and collapse.

The sequence of images in figure 4 shows that the cracking process is similar to that of Test 1. When the water content decreased from 94.2 % (Figure 4a) to 80.1 % (Figure 4b). The first cracks begin to appear on the surface of the sample along with contraction of the soil radiating through the interior with greater intensity. The appearance of the first cracks occurs after 8.8 h of drying, a longer time than in Test 1 because of the higher initial water content. Soil detachment from the Petri dish becomes evident at a water content level of 70.10 %, registering a CIF of 4.0 %, as shown in figure 4c. The sequential crack pattern was similar to that in the previous test, occurring simultaneously across the surface in X- and Y-shapes, forming

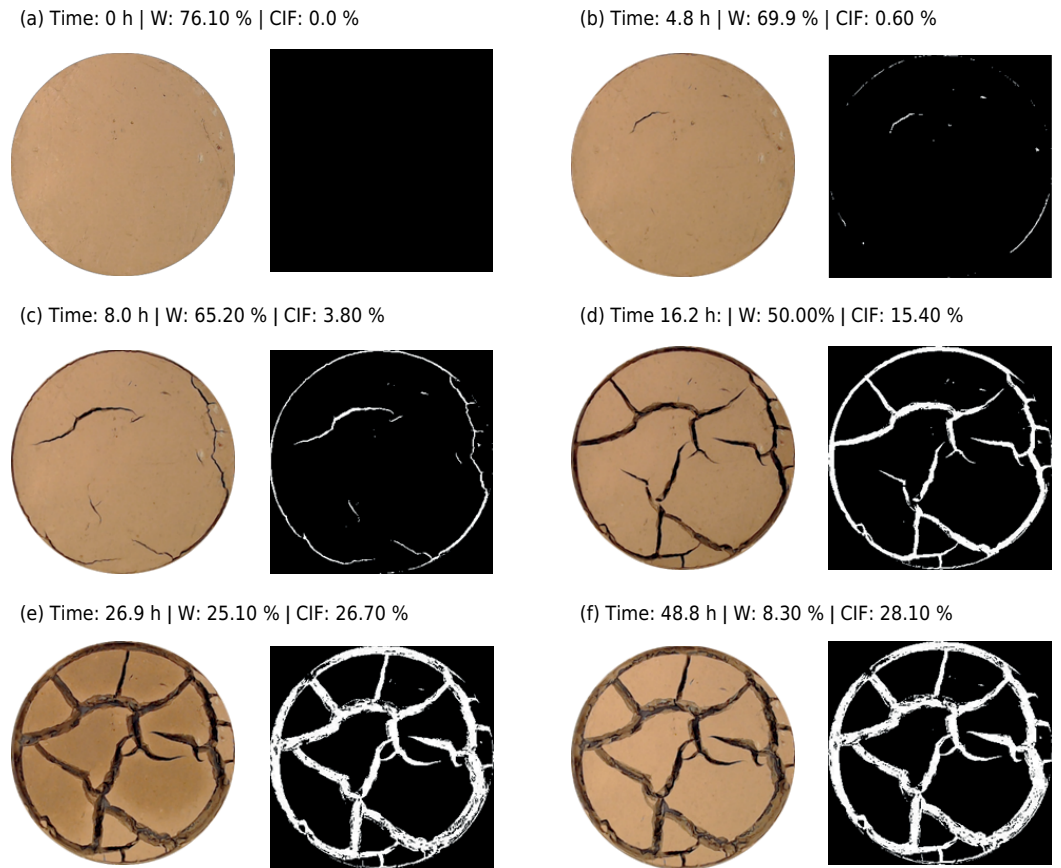


Figure 3. Process of crack development: Test 1 - $W_i = 76.1$ %.

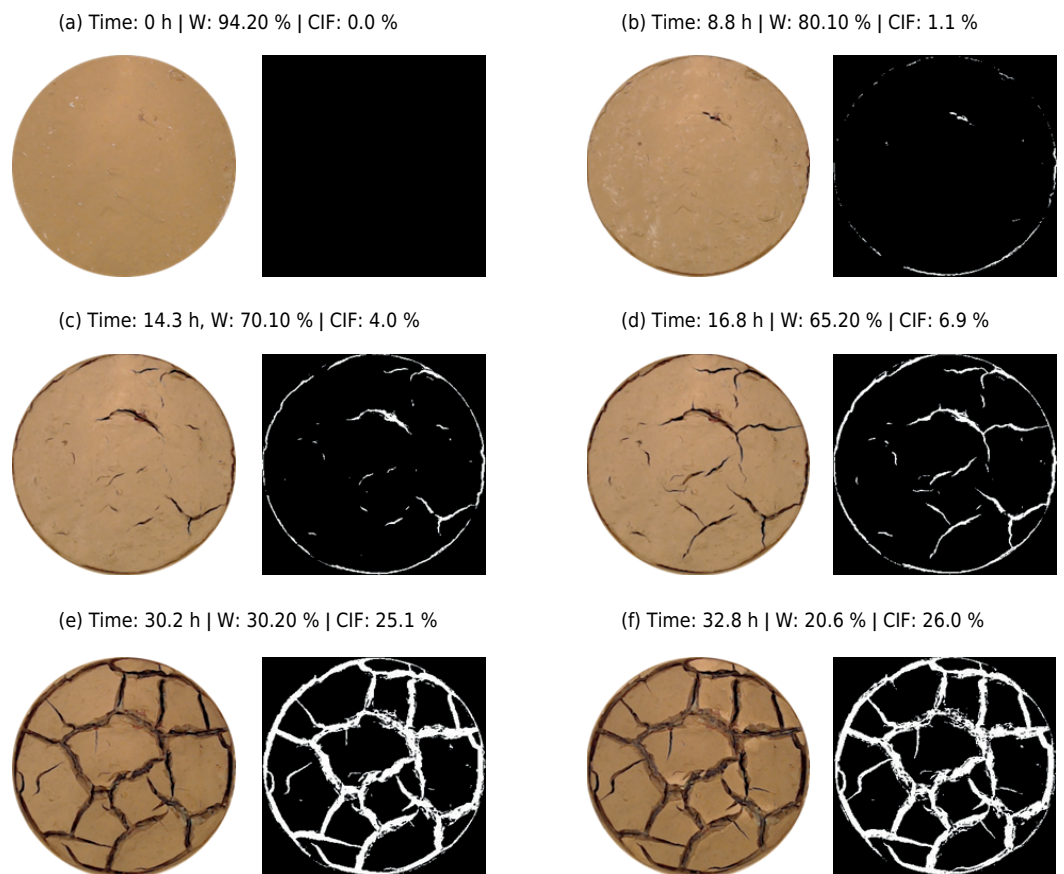


Figure 4. Process of crack development: Test 2 - $W_i = 94.20$ %.

quadrilateral geometric elements (Figures 4d and 4e). However, in this case, there is a greater number of crack plates than in Test 1, as seen in figure 3e. The increase in the CIF factor occurred gradually throughout the test, reaching a maximum value of 26.0 % at the end of the first drying cycle, figure 4f.

After the first drying in Test 2, two more wetting and drying cycles were performed. Figure 5 shows the sample images at the beginning of the test and at the end of each cycle. Figure 6 shows the variation in CIF and water content during the drying and wetting process. The soil had no cracks in its initial condition, with water content of 94.20 % (Figure 5a). At the end of the first drying cycle (32.8 h from the beginning of the test), the soil had a CIF of 28.6 % and water content of 20.60 % (Figure 5b). As the soil is wetted, the suction decreases, the soil expands, and particles from the soil surface move into the cracks, partially closing them. After one hour of wetting, the CIF value strongly decreased, followed by continued slight decreases over time (Figure 6a). At the end of the wetting process, after 103 h (Figure 5c), the water content reached 62 % and the CIF reached 14.6 % (Figure 6b). As the second drying cycle began, water content decreased and CIF increased. At the end of this cycle, after 131 h (Figure 5d), water content was at 26.30 % with a CIF of 22.5 %. A final wetting cycle began, with the soil expanding again, surface particles moving into the cracks to partially close them. At the end of this process, after 200 h (Figure 5e), the water content reached 62 % and the CIF was at 10.6 % (Figure 6). At the end of the drying process, 245.2 h from the beginning of the test (Figure 5f), the water content was 3.30 %, and the CIF 15.9 %.

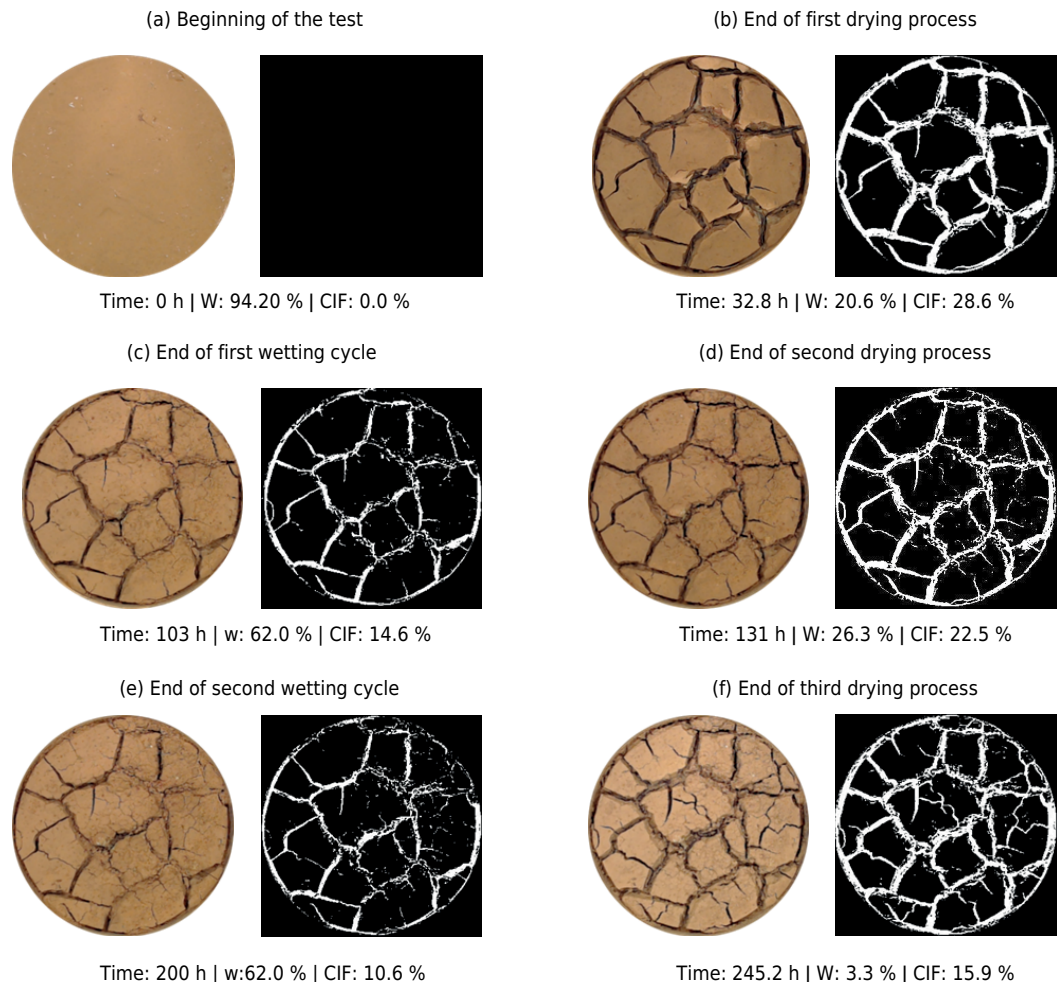


Figure 5. Comparison of images of the cracking process at the beginning and end of each cycle - W_i: 94.20 %.

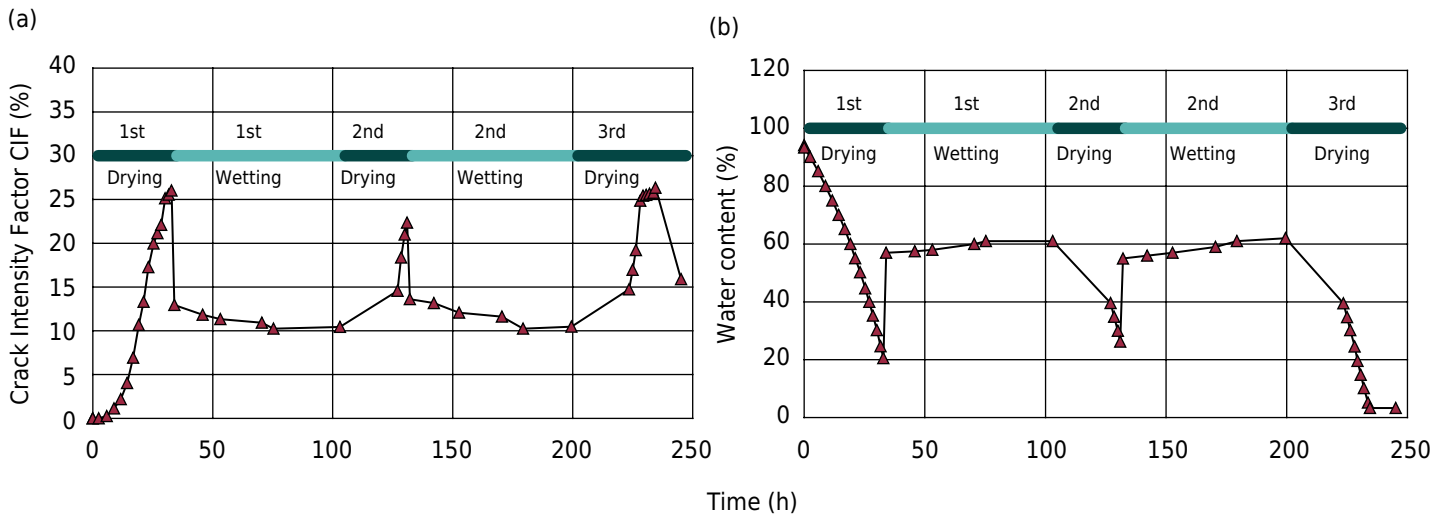


Figure 6. Variation of the Crack Intensity Factor and Water content with Time (a) CIF vs Time, (b) Water content vs Time.

DISCUSSIONS

Volume change behavior due to wetting

Soil swelling decreases as the applied stress increases, indicating that the expansion will be larger when the tension decreases, as shown in figure 2a. For stresses equal to or greater than 160 kPa, the soil no longer expands with increased water content, but compresses instead. Under field water content conditions, the soil experiences a suction of 2.0 MPa and average swelling stress of 169 kPa. Due to the process of soil formation (sedimentary), its particles are oriented in the form of flakes. As water comes into contact with the soil, adsorption forces and osmotic stress cause double-layer plate expansion to occur, with reduced suction and progressive swelling as water comes into contact with the soil, changing it into a dispersed structure as a function of the vertical tension it was subjected to before wetting. Because wetting occurs in a particular direction and the soil has low permeability, the part of the soil in contact with the draining surface begins the expansion process first, before it spreads to the inner part of the sample. Already moistened soil has greater compressibility than the central core of the sample, whose structure is not initially altered.

The variation in the structure during the wetting process as a function of the tension that it is subjected to leads to three possible situations that must be considered: (i) when the applied vertical stress is less than the ground swelling stress, wetting will cause expansion resulting in a greater expansion, the smaller the stress; (ii) when the applied vertical stress is greater than the ground swelling stress, the particles tend to orient themselves when wetted; soil compressibility progressively increases from the periphery to the center of the sample and, as the applied stress is greater than that from swelling, the soil compresses; (iii) when the applied vertical stress is almost the same as the swelling stress, the wetting initially causes a water content change only near the draining surface, altering the compressibility of the soil in this region, and the double layer expansion occurs partially, as in earlier cases, with the effect of applied stress on soil compression initially prevailing. As the wetting front advances, the volume of moist soil increases, and swelling begins to prevail over the effect of applied stress. The deformation measured in the test during the process is the result of the compression because of the applied stress (in the new more compressible dispersed structure) under the swelling stress of the double layer, or vice versa.

The soil swelling stress, obtained by Method 1 (loading after expansion with different overloads; figure 2b), depends on the stress trajectory before wetting, especially for lower values of applied vertical stress. On the other hand, if the wetting takes place

afterward, as in Method 2 (Expansion and Collapse; Figure 2c), or simultaneously, as in Method 3 (Constant Volume), the swelling will only partially occur because it is under stress, leading to lower water content levels. Different values for swelling stress were also obtained in the expansive clay in the La Paz de Arahall Barrier Clay (Serilla, Spain) by Delgado (1986) and Petrolândia Clay (Pernambuco, Brazil) by Ferreira and Ferreira (2009).

Figure 7 shows the variation in the swelling stress obtained by the constant volume method and the contraction rate of undisturbed samples that are subject to different initial suctions. The values for swelling stress and shrink rate increased up to a suction of 33 MPa. For higher values, the swelling stress increased slightly, while the contraction rate decreased slightly, trending towards stabilization. The loss of soil water content increased swelling stress. Ferreira and Ferreira (2009) commented that the previous moistening of the soil causes a reduction in the swelling stress while drying causes an increase. This shows that, in the field, climatic conditions have a significant influence on the soil's swelling stress.

Continuous evaporation of water produces a water-air meniscus between the clay particles and the capillary suction on the outer particle layer. Capillary suction and effective stress between clay particles increase as the soil dries, resulting in soil consolidation and contraction. This process raises the ground swelling stress and the contraction rate, as shown in figure 7. Because the soil has a heterogeneous microstructure conditioned by intrinsic and extrinsic factors, cracks are prone to begin at critical points on the surface, where tensile stress accumulation induced by suction exceeds the soil's tensile strength. Water evaporation plays a significant role in the appearance and growth of cracks during the soil desiccation process.

Crack formation and propagation during soil drying

Figure 8 shows the variation in the mean values of the geometric crack indices, including: CIF, average crack width, total crack length, number of crack segments, and the crack area along the sample surface, as water content decreased for Test 1 (Figure 8a) and Test 2 (Figure 8b). These rates increased initially as water content decreased, and then began to drop. This implies that clay soils tend to crack more easily when the water content is high and that the shrinkage and cracking potential attenuates with decreasing water content. Similar behavior in clay soil was found by Tang et al. (2011c, 2019). For water content above the liquidity limit (Test 2) and above 70 % (Test 1), the geometric

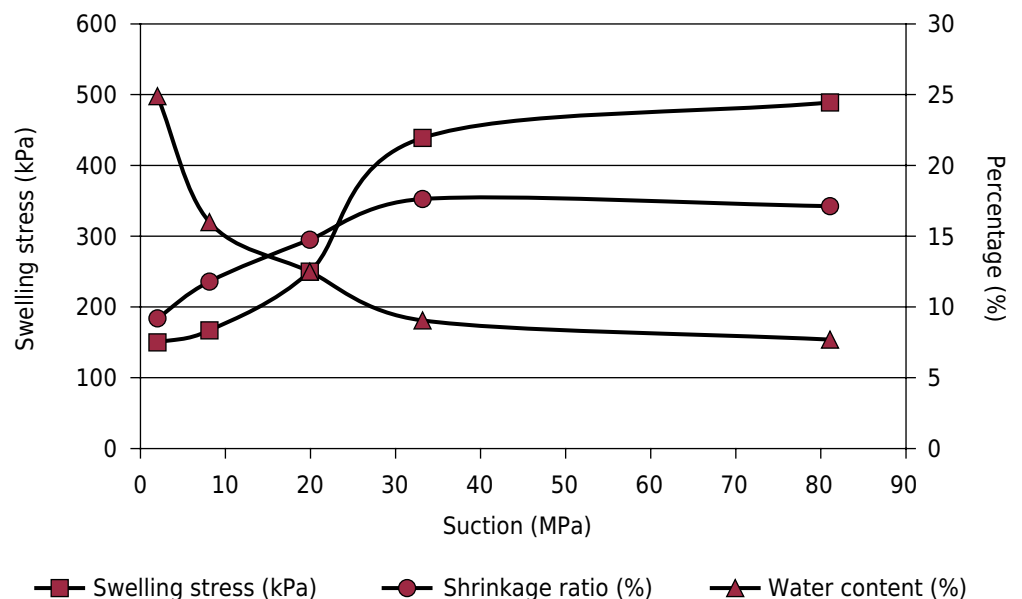


Figure 7. Variation of swelling stress, water content, and shrinkage ratio with suction.

crack indices grow more slowly. For water content between 70 and 30 % (Test 1) and between 70 and 20 % (Test 2), there is a significant increase in the geometric crack indices. For water content lower than the lower limits mentioned above, the geometric crack indices tend to stabilize or decrease as the sample dries, except for the crack indices and crack widths in Test 2, which grew. This is due to the drying and wetting cycle, as will be discussed below.

Clay soil contraction and the resulting cracks are closely related to the amount of clay minerals present and the ease of absorbing or dissolving water. Increased clay content, especially montmorillonite, contributes significantly to this soil contraction behavior (Tay et al., 2001; Vogel et al., 2005). In the soil tested, montmorillonite and illite are

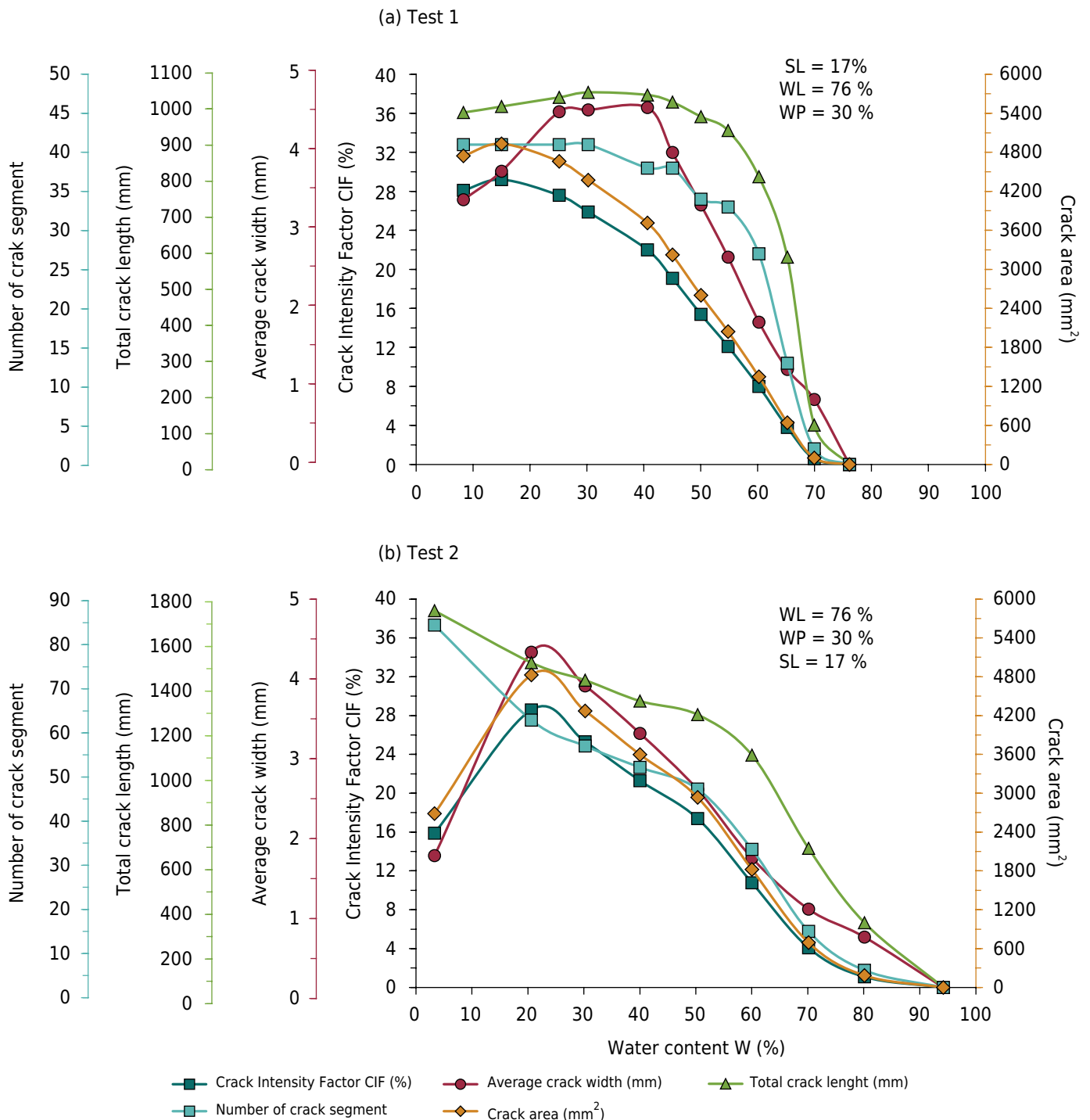


Figure 8. Quantitative evolution of geometric crack indexes while drying.

present, and a strong volumetric shrinkage behavior is observed during the drying process. The hydration film covering the surface of the clay particles becomes thinner as the soil dries. Increased capillary suction decreases the thickness of the film, reducing the pore space between the particles and rearranging the alignment of the particles, reflected in an overall macroscopic volume reduction.

Crack formation and propagation during drying and wetting cycles

Figure 9 shows the influence of the drying and wetting process on the geometric crack index values. The length and number of crack segments increase while the crack width and area decrease with an increasing number of drying and wetting cycles. The reduction in CIF during wetting is due to soil hydration with a double layer expansion that increases basal spacing, as well as displacement of surface particles into the cracks, as shown in figure 5. Particles partially fill cracks with a finer textured material pushed into the soil

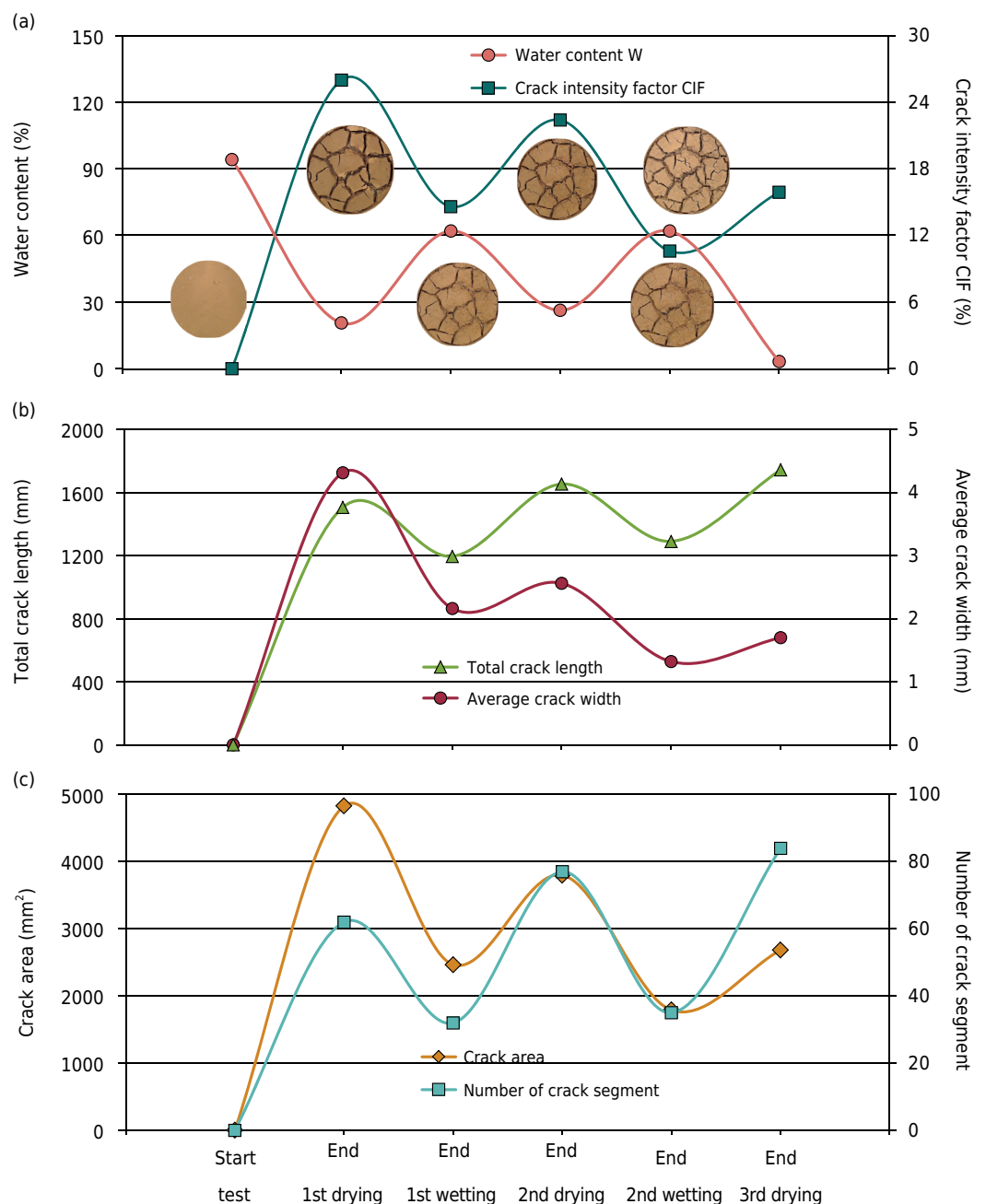


Figure 9. Variation of geometric crack indexes with drying and wetting cycles.

matrix due to the action of high activity clay, forming papules, Brewer (1976), Bullock et al. (1985), and Ferreira (1995). After wetting, new cracks appear with each new drying cycle. These new micro cracks emerged from the existing cracks, interconnecting them. In the last drying cycle, there was a change of soil coloration due to water loss, becoming quite evident at the end of the test when soil water content passed below 15 %.

Comparison of expansion deformation curves due to wetting and CIF due to drying over time

The expansion deformation process (on a logarithmic scale) due to wetting under constant applied external stress (to 10 kPa; Figure 10) can be divided into three stages: (a) initial expansion - for times shorter than three minutes, water is adsorbed by the clay during a wetting cycle and the soil becomes a cohesive mass with small expansion deformations observed in the soil; water moistens only the periphery (Figure 10a); (b) primary expansion - for times between three and 160 min, water percolates from the periphery towards the center, progressively moistening the soil and expansion occurs with greater intensity; the soil becomes more plastic and sticky, as in figures 10b and 10c and in extreme cases only a very fine granular structure remains; (c) secondary expansion - for times longer than 160 minutes; water moistens the central core, the voids are almost filled with water and the rate of deformation decreases (Figure 10d). Similar behavior was observed by Ferreira and Ferreira (2009). Rao (2006) considered the initial deformations to be associated with the microstructure, and the primary and secondary deformations to be associated with the macrostructure.

The crack propagation process shown by the CIF versus time curve also has three stages: initial, primary, and secondary cracks (Figure 11). In the initial crack stage, up to 4.8 h, the water content loss rate is low (1.20 \% h^{-1}) and significant cracking does not appear ($\text{CIF} = 3.8 \text{ \%}$). The primary cracking stage begins after 4.8 h and extends until there the CIF stabilizes around 29.5 h, with a 26.9 % CIF and a water content loss rate of 2.64 \% h^{-1} . The last stage, that of secondary cracking, begins when primary cracking ends and extends to the completion of the test, with a water content loss rate of 0.37 \% h^{-1} and a tendency for residual water content and CIF. Similar behavior was observed by Tang et al. (2011c).

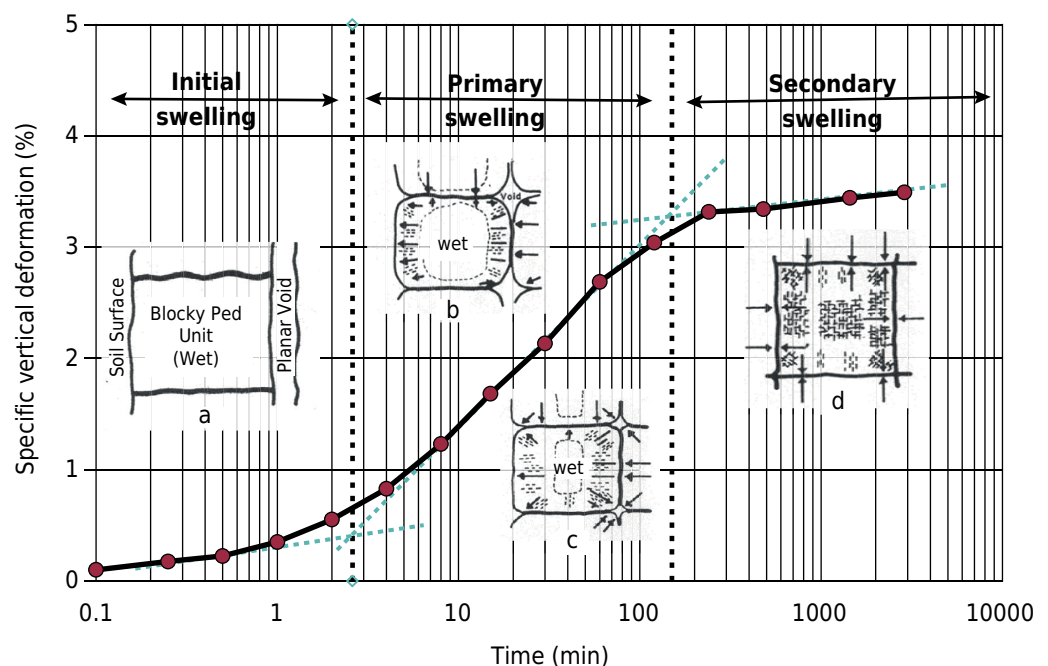


Figure 10. Soil behavior during expansion.

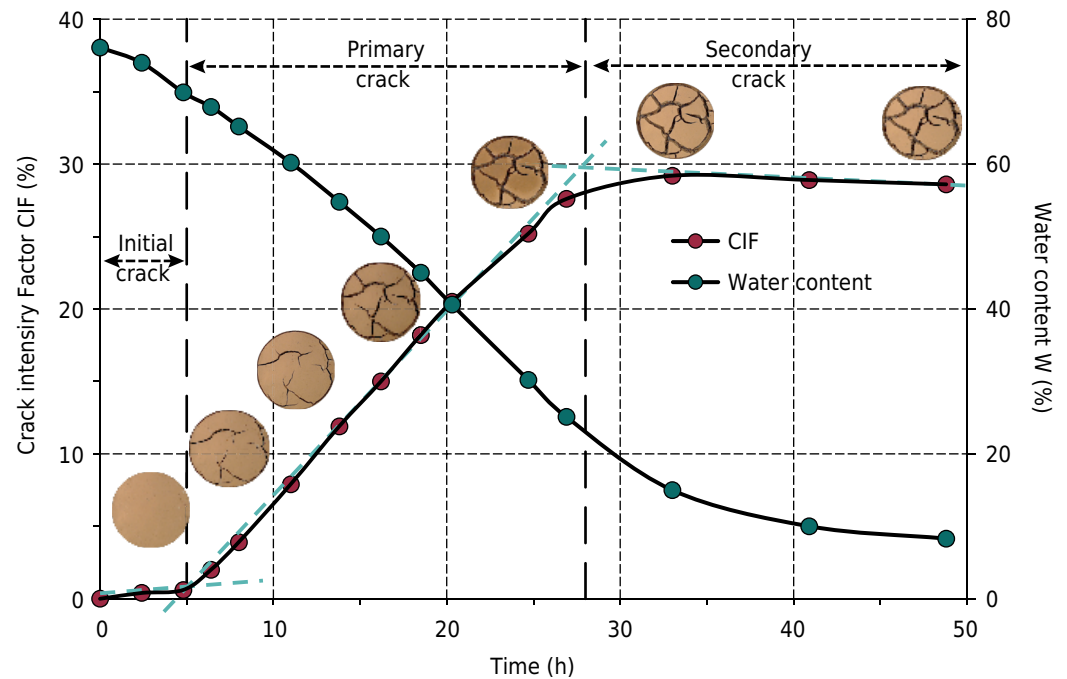


Figure 11. Soil behavior during crack propagation.

The volume variation process due to wetting and the crack propagation process due to drying over time has three distinct stages: initial, primary, and secondary, as shown in the expansion deformation vs. time curve during wetting (Figure 10) and the CIF vs. time curve during drying (Figure 11).

CONCLUSIONS

Swelling deformation due to wetting is a function of the suction, structure, and applied stress to the soil prior to wetting. Thus, the resulting measures found over time are expansion, expansion and compression, or just compression.

The fundamental difference between the determination of swelling stress methods is the order in which stress is applied and wetting. The device developed to evaluate the process of crack propagation using a scale, webcam, lamps, and hygrometer, in an environment that permits only small variations of temperature and relative air water content, performed adequate.

The crack propagation tests showed that X or Y shaped cracks formed initially, followed by other cracks originating as branches from the first ones. As the water content approached the soil contraction limit, the crack development slowed and approached a secondary stage of propagation.

Expansive clay soils tend to crack more easily at higher water contents and the crack attenuates with decreasing water. Increasing rates of increase in geometric crack indices occurred more rapidly during the primary stage of water evaporation and subsequently decreased with continuous water loss in the secondary stage. With each drying and wetting cycle, new cracks appear. The new cracks branched off from the already existing cracks, interconnecting them with each other.

ACKNOWLEDGMENTS

We thank CNPq for supporting the development of the research Process: 421087/2018-8 and for the scholarship.

AUTHOR CONTRIBUTIONS

Conceptualization:  Silvio Romero de Melo Ferreira (lead),  Arthur Gomes Dantas Araújo (lead),  Felipe Araújo Silva Barbosa (supporting),  Thalita Cristina Rodrigues Silva (supporting), and  Izabela Medeiros Lima Bezerra (supporting).

Methodology:  Silvio Romero de Melo Ferreira (lead),  Arthur Gomes Dantas Araújo (lead),  Felipe Araújo Silva Barbosa (equal),  Thalita Cristina Rodrigues Silva (equal), and  Izabela Medeiros Lima Bezerra (equal).

Software:  Silvio Romero de Melo Ferreira (equal),  Arthur Gomes Dantas Araújo (lead),  Felipe Araújo Silva Barbosa (equal),  Thalita Cristina Rodrigues Silva (equal), and  Izabela Medeiros Lima Bezerra (equal).

Validation:  Silvio Romero de Melo Ferreira (lead),  Arthur Gomes Dantas Araújo (lead),  Felipe Araújo Silva Barbosa (supporting),  Thalita Cristina Rodrigues Silva (supporting), and  Izabela Medeiros Lima Bezerra (equal).

Formal analysis:  Silvio Romero de Melo Ferreira (lead),  Arthur Gomes Dantas Araújo (equal),  Felipe Araújo Silva Barbosa (equal),  Thalita Cristina Rodrigues Silva (equal), and  Izabela Medeiros Lima Bezerra (equal).

Investigation:  Silvio Romero de Melo Ferreira (lead),  Arthur Gomes Dantas Araújo (lead),  Felipe Araújo Silva Barbosa (supporting),  Thalita Cristina Rodrigues Silva (supporting), and  Izabela Medeiros Lima Bezerra (supporting).

Resources:  Silvio Romero de Melo Ferreira (lead),  Arthur Gomes Dantas Araújo (lead),  Felipe Araújo Silva Barbosa (supporting),  Thalita Cristina Rodrigues Silva (supporting), and  Izabela Medeiros Lima Bezerra (supporting).

Data curation:  Silvio Romero de Melo Ferreira (lead),  Arthur Gomes Dantas Araújo (equal),  Felipe Araújo Silva Barbosa (equal),  Thalita Cristina Rodrigues Silva (supporting), and  Izabela Medeiros Lima Bezerra (supporting).

Writing - original draft:  Silvio Romero de Melo Ferreira (equal),  Arthur Gomes Dantas Araújo (lead),  Felipe Araújo Silva Barbosa (equal),  Thalita Cristina Rodrigues Silva (supporting), and  Izabela Medeiros Lima Bezerra (supporting).

Writing - review and editing:  Silvio Romero de Melo Ferreira (lead),  Arthur Gomes Dantas Araújo (equal),  Felipe Araújo Silva Barbosa (supporting),  Thalita Cristina Rodrigues Silva (supporting), and  Izabela Medeiros Lima Bezerra (supporting).

Visualization:  Silvio Romero de Melo Ferreira (lead),  Arthur Gomes Dantas Araújo (equal),  Felipe Araújo Silva Barbosa (supporting),  Thalita Cristina Rodrigues Silva (supporting), and Izabela Medeiros Lima Bezerra (supporting).

Supervision:  Silvio Romero de Melo Ferreira (lead),  Arthur Gomes Dantas Araújo (equal),  Felipe Araújo Silva Barbosa (supporting),  Thalita Cristina Rodrigues Silva (supporting), and  Izabela Medeiros Lima Bezerra (supporting).

Project administration:  Silvio Romero de Melo Ferreira (lead),  Arthur Gomes Dantas Araújo (equal),  Felipe Araújo Silva Barbosa (supporting),  Thalita Cristina Rodrigues Silva (supporting), and  Izabela Medeiros Lima Bezerra (supporting).

Funding acquisition:  Silvio Romero de Melo Ferreira (lead),  Arthur Gomes Dantas Araújo (equal),  Felipe Araújo Silva Barbosa (supporting),  Thalita Cristina Rodrigues Silva (supporting), and  Izabela Medeiros Lima Bezerra (supporting).

REFERENCES

- Albrecht BA, Benson CH. Effect of desiccation on compacted natural clay. *J Geotech Geoenviron.* 2001;127:67-75. [https://doi.org/10.1061/\(ASCE\)1090-0241\(2001\)127:1\(67\)](https://doi.org/10.1061/(ASCE)1090-0241(2001)127:1(67))
- Albright WH, Benson CH, Gee GW, Abichou T, McDonald EV, Tyler SW, Rock AS. Field performance of a compacted clay landfill final cover at a humid site. *J Geotech Geoenviron.* 2006;132:1393-403. [https://doi.org/10.1061/\(ASCE\)10900241\(2006\)132:11\(1393\)](https://doi.org/10.1061/(ASCE)10900241(2006)132:11(1393))
- Al-Mukhtar M, Khattab S, Alcover JF. Microstructure and geotechnical properties of lime-treated expansive clayey soil. *Eng Geol.* 2012;139-140:17-27. <https://doi.org/10.1016/j.enggeo.2012.04.004>
- Al-Rawas AA, Goosen MFA, Al-Rawas GA. Geology, classification and distribution of expansive soils and rocks. In: Al-Rawas AA, Goosen MFA, editors. *Expansive soils: Recent advances in characterization and treatment.* London: Taylor & Francis Group; 2006. p. 3-14.
- Ammour A, Bouhanna B. Contribution a L'etude de la fissuration des argiles [dissertation]. Tlemcen: Université de Tlemcen; 2016.
- Antunes FS, Salomão FXT. Solos em pedologia. In: Oliveira MAS, Monticeli JJ, editores. *Geologia de engenharia e ambiental.* São Paulo: Associação Brasileira de Geologia e Ambiental; 2018. vol. 2. p. 71-85.
- Atique A, Sanchez M. Analysis of cracking behavior of drying soil. In: 2nd International Conference on Environmental Science and Technology; 2011 Feb 26-28; Singapore. Singapore: International Proceedings of Chemical, Biological and Environmental Engineering; 2011. p. 66-70.
- Bastos EG. Variação volumétrica de uma argila expansiva do litoral norte de Pernambuco [dissertação]. Campina Grande: Universidade Federal da Paraíba; 1994.
- Biasus M, Pauletto EA, Crestana S. Estudo da deformação de um Vertissolo por meio da tomografia computadorizada de dupla energia simultânea. *Rev Bras Cienc Solo.* 1999;23:1-7. <https://doi.org/10.1590/S0100-06831999000100001>
- Brewer R. *Fabric and mineral analysis of soils.* New York: Krieger; 1976.
- Bullock P, Federoff N, Jongerius A, Stoops G, Tursina T. *Handbook for soil thin section description.* London: Waine Research Publications; 1985.
- Chaduvula U, Viswanadham BVS, Kodikara J. A study on desiccation cracking behavior of polyester fiber-reinforced expansive clay. *Appl Clay Sci.* 2017;142:163-72. <https://doi.org/10.1016/j.clay.2017.02.008>
- Chaduvula U, Viswanadham BVS, Kodikara J. Desiccation cracking behavior of geofiber-reinforced expansive clay. In: *Geo-Chicago 2016 Sustainable Geoenvironmental Systems;* 2016 Aug 14-18; Chicago, EUA. Reston: American Society of Civil Engineers Library ASCE; 2016. p. 368-77.
- Chen FH. *Foundations on expansive soils.* 2nd ed. Amsterdam: Elsevier Scientific Publishing Co.; 1988.
- Climate-data.Org. Dados climáticos para cidades mundiais [internet]. São Paulo: Climate-Data.org / AM OP / OpenStreetMap contributors; 2019 [cited 2019 April 10]. Available from: <https://pt.climate-data.org/america-do-sul/brasil/pernambuco/paulista-4450/>.
- Collares GL, Reinert DJ, Reichert JM, Kaiser DR. Compactação de um Latossolo induzida pelo tráfego de máquinas e sua relação com o crescimento e produtividade de feijão e trigo. *Rev Bras Cienc Solo.* 2008;32:933-42. <https://doi.org/10.1590/S0100-06832008000300003>
- Corrêa MM, Ker JC, Mendonça ES, Ruiz HA, Bastos RS. Atributos físicos, químicos e mineralógicos de solos da região das várzeas de Sousa (PB). *Rev Bras Cienc Solo.* 2003;27:311-24. <https://doi.org/10.1590/S0100-06832003000200011>
- Cotecchia F, Vitone C. Behavioural features of fissured clays: experimental evidence and modelling. In: 6th International Symposium on Deformation Characteristics of Geomaterials; 2015 Nov 15-18; Buenos Aires, Argentina. Amsterdam: IOS Press; 2015. p. 615-22.

- Delgado A. Influencia de la trayectoria de las tensiones en el comportamiento de las arcillas expansivas y de los suelos colapsables en el laboratorio y en el terreno [thesis]. Sevilla: Universidad de Sevilla; 1986.
- Ferreira SRM. Colapso e expansão de solos naturais não saturados devidos à inundação [thesis]. Rio de Janeiro: Universidade Federal do Rio de Janeiro; 1995.
- Ferreira SRM, Ferreira MGVX. Mudanças de volume devido a variação de teor de umidade em um Vertissolo no semiárido de Pernambuco. *Rev Bras Cienc Solo*. 2009;33:779-91. <https://doi.org/10.1590/S0100-06832009000400004>
- Ferreira SRM, Paiva SC, Morais JJO, Viana RB. Avaliação da expansão de um solo do município de Paulista-PE melhorado com cal. *Materia*. 2017;22:e11930. <https://doi.org/10.1590/s1517-707620170005.0266>
- Fleureau JM, Wei X, Ighil-Ameur L, Hattab M, Bicalho KV. Experimental study of the cracking mechanisms of clay during drying. In: 15th Pan-American Conference on Soil Mechanics and Geotechnical Engineering; 2015 Nov 15-18; Buenos Aires, Argentina. Amsterdam: IOS Press; 2015. p. 2101-8.
- Flores JPC, Anghinoni I, Cassol LC, Carvalho PCF, Leite JGDB, Fraga TI. Atributos físicos do solo e rendimento de soja em sistema plantio direto em integração lavoura-pecuária com diferentes pressões de pastejo. *Rev Bras Cienc Solo*. 2007;31:771-80. <https://doi.org/10.1590/S0100-06832007000400017>
- Ghazizade MJ, Safari E. Analysis of desiccation crack depth in three compacted clay liners exposed to annual cycle of atmospheric conditions with and without a geotextile cover. *J Geotech Geoenviron*. 2017;143:06016024. Technical Note. [https://doi.org/10.1061/\(ASCE\)GT.1943-5606.0001607](https://doi.org/10.1061/(ASCE)GT.1943-5606.0001607)
- Julina M, Thyagaraj T. Determination of volumetric shrinkage of an expansive soil using digital camera images. *Int J Geotech Eng*. 2018;12:1-9. <https://doi.org/10.1080/19386362.2018.1460961>
- Lakshmikantha MR, Prat PC, Ledesma A. Image analysis for the quantification of a developing crack network on a drying soil. *Geotech Test J*. 2009;32:505-15. <https://doi.org/10.1520/GTJ102216>
- Lambe TW, Whitman RV. *Soil mechanics*. New York: John Wiley & Sons; 1969.
- Li JH, Zhang LM. Study of desiccation crack initiation and development at ground surface. *Eng Geol*. 2011;123:347-58. <https://doi.org/10.1016/j.enggeo.2011.09.015>
- Li JH, Zhang LM. Geometric parameters and REV of a crack network in soil. *Comput Geotech*. 2010;37:466-75. <https://doi.org/10.1016/j.compgeo.2010.01.006>
- Li XW, Wang Y, Yu JW, Wang YL. Unsaturated expansive soil fissure characteristics combined with engineering behaviors. *J Cent South Univ*. 2012;19:3564-71. <https://doi.org/10.1007/s11771-012-1444-0>
- Lim BF, Siemens GA. Unifying framework for modeling swelling soil behaviour. *Can Geotech J*. 2016;53:1495-509. <https://doi.org/10.1139/cgj-2015-0049>
- Liu X, Buzzi O, Vaunat J. Influence of stress-volume path on swelling behavior of an expansive clay. In: Khalili N, Russell A, Khoshghalb A, editors. *Unsaturated soils: research and applications*. Leiden: CRC Press; 2014. p. 931-7.
- Lloret A, Ledesma A, Rodríguez R, Sanchez MJ, Olivella S, Surlol J. Crack initiation in drying soils. In: 2nd International Conference on Unsaturated Soils; 1998 Aug 27-30; Beijing, China. Beijing: International Academic Publishers; 1998. p. 497-502.
- Marques FA, Souza RAS, Souza JES, Lima JFWF, Souza Júnior VS. Caracterização de Vertissolos da ilha de Fernando de Noronha, Pernambuco. *Rev Bras Cienc Solo*. 2014;38:1051-65. <https://doi.org/10.1590/S0100-06832014000400002>
- Mitchell JK. *Fundamentals of soil behaviour*. 3rd ed. New York: John Wiley & Sons; 1976.
- Moraes MT, Debiasi H, Franchini JC, Silvan VR. Propriedades físicas do solo sob diferentes níveis de compactação em um Latossolo Vermelho distroférrico. In: *Jornada acadêmica da Embrapa Soja*; 2011; Londrina, Brasil. Londrina: Embrapa Soja; 2011. p. 51-5. (Documentos 328).

- Munsell Color Company. Munsell soil color charts. New Windsor: Kollmorgen Instruments - Macbeth Division; 1992.
- Nahlawi H, Kodikara JH. Laboratory experiments on desiccation cracking of thin soil layers. *Geotech Geol Eng.* 2006;24:1641-64. <https://doi.org/10.1007/s10706-005-4894-4>
- Rao SM. Identification and classification of expansive soils. In: Al-Rawas AA, Gossen MFA, editors. *Expansive soils: recent advances in characterization and treatment.* London: Taylor & Francis Group; 2006. p. 15-24.
- Rodríguez R, Sánchez M, Ledesma A, Lloret A. Experimental and numerical analysis of desiccation of a mining waste. *Can Geotech J.* 2007;44:644-58. <https://doi.org/10.1139/T07-016>
- Sánchez M, Manzoli OL, Guimarães LJM. Modeling 3-D desiccation soil crack networks using a mesh fragmentation technique. *Comput Geotech.* 2014;62:27-39. <https://doi.org/10.1016/j.compgeo.2014.06.009>
- Shi B, Chen S, Han H, Zheng C. Expansive soil crack depth under cumulative damage. *Sci World J.* 2014;2014:1-14. <https://doi.org/10.1155/2014/498437>
- Tang AM, Vu MN, Cui YJ. Effects of the maximum soil aggregates size and cyclic wetting-drying on the stiffness of a lime-treated clayey soil. *Geotechnique.* 2011c;61:421-9. <https://doi.org/10.1680/geot.SIP11.005>
- Tang CS, Cui YJ, Shi B, Tang AM, Liu C. Desiccation and cracking behavior of clay layer from slurry state under wetting-drying cycles. *Geoderma.* 2011a;66:111-8. <https://doi.org/10.1016/j.geoderma.2011.07.018>
- Tang CS, Cui YJ, Tang AM, Shi B. Experimental evidence on the temperature dependence of desiccation cracking behavior of clayey soils. *Eng Geol.* 2010;114:261-6. <https://doi.org/10.1016/j.enggeo.2010.05.003>
- Tang CS, Shi B, Liu C, Suo WB, Gao L. Experimental characterization of shrinkage and desiccation cracking in thin clay layer. *Appl Clay Sci.* 2011b;52:69-77. <https://doi.org/10.1016/j.clay.2011.01.032>
- Tang CS, Zhu C, Leng T, Shi B, Cheng Q, Zeng H. Three-dimensional characterization of desiccation cracking behavior of compacted clayey soil using X-ray computed tomography. *Eng Geol.* 2019;255:105212. <https://doi.org/10.1016/j.enggeo.2019.04.014>
- Tay YY, Stewart DI, Cousens TW. Shrinkage and desiccation cracking in bentonite-sand landfill liners. *Eng Geol.* 2001;60:263-74. [https://doi.org/10.1016/S0013-7952\(00\)00107-1](https://doi.org/10.1016/S0013-7952(00)00107-1)
- Vijayvergiya VN, Ghazzaly OI. Prediction of swelling potential for natural clays. In: *Proceedings of the 3rd International Conference on Expansive Soils; 1973 July 30-August 1; Haifa.* Jerusalem: Academic Press; 1973. vol. 1. p. 227-36.
- Vogel HJ, Hoffmann H, Roth K. Studies of crack dynamics in clay soil I. experimental methods, results, and morphological quantification. *Geoderma.* 2005;125:203-11. <https://doi.org/10.1016/j.geoderma.2004.07.009>
- Yuan S, Liu X, Sloan SW, Buzzi OP. Multi-scale characterization of swelling behaviour of compacted Maryland clay. *Acta Geotech.* 2016;11:789-804. <https://doi.org/10.1007/s11440-016-0457-5>